

Stability of InAs quantum dots

Ch. Heyn*

Institut für Angewandte Physik und Zentrum für Mikrostrukturforschung, Jungiusstrasse 11, D-20355 Hamburg, Germany

(Received 7 November 2001; revised manuscript received 9 January 2002; published 2 August 2002)

We monitor the postgrowth desorption of self-assembled InAs quantum dots with electron diffraction. A kinetic model is presented that quantitatively describes the temperature and arsenic pressure dependence of the postgrowth dot lifetimes. The central findings establish the stabilization of the InAs quantum dots by an arsenic flux, the importance of the precursor state for the impinging arsenic molecules, and layer-by-layer desorption starting from the dot-top. In a second step the model results are employed to refine the description of the growth process providing a now complete picture of the here relevant desorption mechanisms. The such calculated sticking coefficient matches quantitatively our temperature-dependent measurements of the critical time up to quantum dot formation.

DOI: 10.1103/PhysRevB.66.075307

PACS number(s): 61.14.Hg, 68.35.Rh, 81.07.-b, 81.15.Hi

Self-assembling mechanisms that enable the controlled generation of crystalline quantum-size structures are a fascinating aspect of physics. A very prominent example are strain-induced InAs quantum dots grown on GaAs in the Stranski–Krastanov mode.¹ Being artificial atoms they intrigue from a fundamental point of view. But self-assembled quantum dots are also very attractive for device applications such as quantum dot lasers. The properties of these quantum dots are crucially dependent on the parameters of the growth procedure.² Applying molecular beam epitaxy (MBE), the central parameters are the temperature, the indium and arsenic flux, and the deposition time. The influence of these parameters is quite complex and is not yet completely resolved. As the most important parameter the temperature controls the surface activity of the adsorbants which is finally responsible for the quantum dot formation,³ the intermixing with gallium from the substrate,^{3–6} and the desorption of atoms from the surface. Until now, very little attention has been paid to the latter process and the influence of the arsenic flux. In this work, we apply *in situ* electron diffraction to study the temperature and arsenic pressure dependence of the desorption process during growth as well as in the post-growth regime. A kinetic desorption model is developed, which demonstrates quantitative reproduction of the experimental data.

The measurements are performed in a solid-source MBE system equipped with a valved-cracker cell for arsenic. In the experiments described here, the cracker temperature is chosen according to As₄ emission and the valve is used to precisely control the As₄ flux in a range corresponding to a flux gauge reading between 1.9×10^{-6} and 1.5×10^{-5} Torr. In order to calibrate the flux-gauge reading, the method described in Ref. 7 is applied. We find an As₄ flux of $7.6 \times 10^{14} \text{ cm}^{-2} \text{ s}^{-1}$ at a flux gauge reading of 5.5×10^{-6} Torr. Under consideration of a maximum As₄ sticking coefficient of 0.5 as in the GaAs system,⁸ one gets an effective As₁ flux to the surface of $F_{\text{As}} \text{ (ML/s)} = 4.5 \times 10^5$ times flux gauge reading (Torr).

Starting from flat (001) oriented GaAs substrates, first a GaAs buffer layer is grown at 600 °C in order to smoothen the surface. Before InAs deposition the growth is interrupted to reduce the growth temperature to 433–548 °C. We study

the InAs quantum dot formation as well as the postgrowth behavior with reflection high-energy electron diffraction (RHEED) using 12-keV electrons. During growth, after the critical time t_C , a transition from a two-dimensional (2D) growth related RHEED pattern at the early stages of deposition to transmission diffraction of three-dimensional (3D) features is found. Inset (a) of Fig. 1 shows a RHEED pattern, typical for 3D quantum dot-like islands, which is recorded directly after deposition of 2.0-ML InAs. The additional intensity tails so-called chevrons that are attached to each spot are attributed to the side-facets of the dots.⁹ Detailed descriptions of the experimental procedure and of RHEED measurements during the InAs quantum dot formation are given in Refs. 3 and 10.

The postgrowth stability of the InAs quantum dots is studied under variation of the temperature T and of the arsenic flux F_{As} . For the arsenic flux dependent desorption experiments, the quantum dots are grown with substrate temperature $T = 518 \text{ °C}$, indium flux $F_{\text{In}} = 0.1 \text{ ML/s}$, InAs coverage $\theta_{\text{In}} = 2.0 \text{ ML}$, and $F_{\text{As}} = 4.8 \text{ ML/s}$. At the end of InAs deposition, the indium shutter is closed and the arsenic flux is adjusted with the valve or even completely stopped by closing the main-shutter in the MBE growth chamber. In the temperature-dependent desorption experiments, the temperature is adjusted prior to the InAs deposition, since a controlled variation of the temperature requires significantly more time than the experimental time scales. In order to obtain a quantitative measure of the time scales relevant during the postgrowth regime, the intensity of a 3D growth related RHEED spot [indicated by the arrow in inset of Fig. 1(a)] is recorded. An example of the measured RHEED time evolution is plotted in Fig. 1. In these measurements, we define the time at which the indium shutter is closed as $t = 0$. We find the general trend that, after a period with nearly constant intensity, the intensity decreases down to the reappearance of a 2D surface morphology.

In a growth model employed previously for lower temperatures, where desorption is not relevant, we expect that during a growth-stop the quantum dot height increases and the diameter slightly shrinks.³ Since this behavior does not explain our RHEED measurements at higher temperatures,

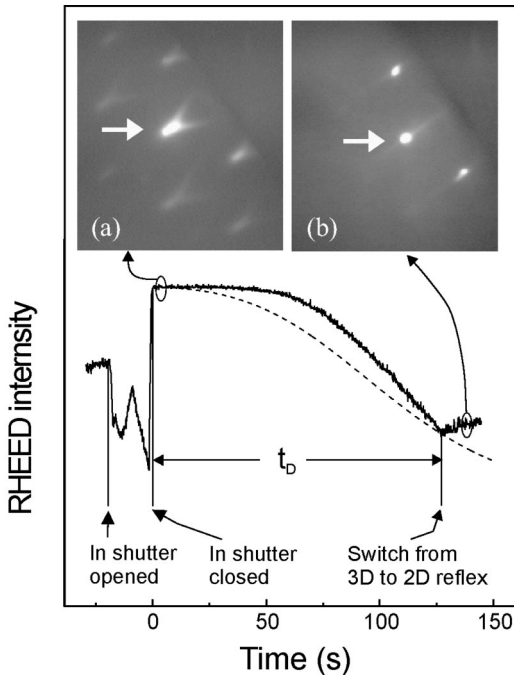


FIG. 1. Time evolution of the RHEED reflex intensity (bulk line) together with the calculated quantum dot volume (dashed line), and the corresponding RHEED patterns. The sudden increase of the RHEED signal prior to the indium shutter closure reflects the 2D to 3D transition. Insets: (a) InAs quantum dots after deposition of 2.0-ML InAs in $[\bar{1}10]$ -azimuth, the arrow points to the 3D-type reflex that is used for the measurement of the time-dependent intensity, (b) 2D morphology in the postgrowth regime 160 s after deposition is stopped, the arrow points to the 2D reflex used for the time-dependent measurements. The 2D pattern reappear after a time t_D . The parameters are $T=524^\circ\text{C}$ and $F_{\text{As}}=4.8$ ML/s.

we attribute our observations to the additional process of desorption and a resulting dissolution of the quantum dots. As a quantitative characterization of the quantum dot lifetime, we define the time t_D up to the instant at which the 3D reflex intensity becomes lower than that of 2D reflexes which now arise. This is observed in the recorded spot intensity as a sharp minimum at cutoff of the monotonous decrease. A corresponding 2D RHEED pattern is shown in inset (b) of Fig. 1. In our experiments, the quantum dot lifetime t_D can be significantly enhanced by a reduction of the temperature (Fig. 2) as well as by a higher arsenic flux (Fig. 3). As an example, at $T=518^\circ\text{C}$, t_D increases from approximately 7 s without arsenic flux to more than 200 s by applying an arsenic flux $F_{\text{As}}=6.0$ ML/s. This result clearly demonstrates the stabilization of the InAs quantum dots by an impinging arsenic flux. From the experimental temperature dependence of t_D at $F_{\text{As}}=0$ we estimate the activation energy $E=3.53$ eV and the prefactor $t_0=2.05\times 10^{-22}$ s assuming Arrhenius type behavior $t_D=t_0\exp(E/k_B T)$, where k_B is Boltzmann's constant. We note the surprising small prefactor similar to the one found in Ref. 11. The physical possibility of such small prefactors has been motivated in Ref. 11. However, a detailed theoretical understanding is not available at present.

To model the above-mentioned experiments, we assume

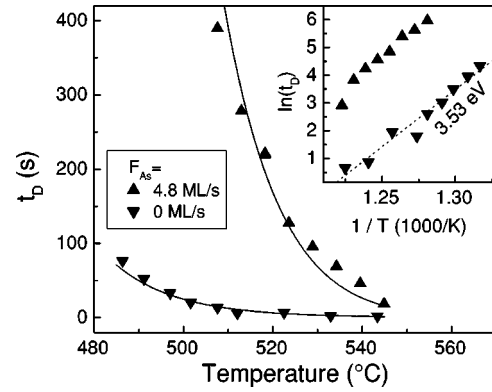


FIG. 2. Measured (symbols) and calculated (line) temperature dependence of the postgrowth quantum dot lifetime t_D . Two values of the arsenic flux are chosen: $F_{\text{As}}=0$ ML/s and $F_{\text{As}}=4.8$ ML/s. The inset shows Arrhenius plots of the data.

that after deposition of 2.0-ML InAs a ML-thick InAs wetting layer has been formed and that the remaining material is accumulated in the quantum dots. From atomic force microscopy, we find a typical dot density of 2.0×10^{10} cm^{-2} corresponding to an average number of 51 900 atoms per dot. Assuming pyramid-shaped dots with volume V_P and an angle¹² α of 26° between the substrate and the pyramid side-facets, the initial pyramid height is $h_P=21$ ML. From diffraction theory, the intensity of a diffracted spot is proportional to the diffracting volume. This establishes the measured time evolution of the 3D RHEED spot in Fig. 1 as an important result, since the initially small and subsequently rapidly increasing desorption rate points out layer-by-layer desorption starting from the pyramid-top instead of re-evaporation from the initially large pyramid side-facets. The quantum dot volume evolution calculated assuming layer-by-layer desorption (see the layer model in the following) provides qualitative reproduction of the time evolution of the RHEED signal in Fig. 1.

In the following, we start with a simple continuum model that allows an analytical treatment of quantum dot desorption, but without consideration of impinging fluxes. An expanded layer based model that includes fluxes of In and As is

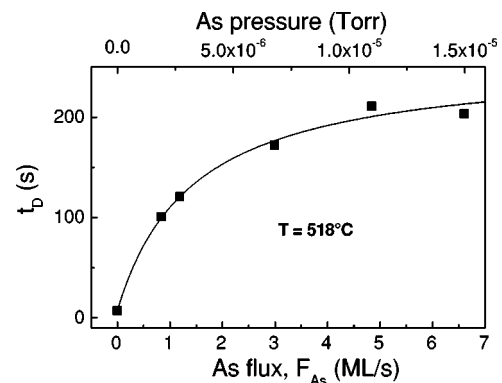


FIG. 3. Dependence of the measured (symbols) and the calculated (line) time t_D on the arsenic flux at a temperature $T=518^\circ\text{C}$.

applied to calculate the stabilization of the dots by arsenic as well as the indium sticking coefficient during growth.

The size of the square area on top of a truncated pyramid with volume V is $A = [6 \cot(\alpha)(V_p - V)]^{2/3}$. An atom of species j may desorb from this area after its lifetime $\tau_j = t_{0,j} \exp(E_j/k_B T)$, where $t_{0,j}$ is a prefactor, and E_j is the energy barrier for desorption. Since for desorption of both species, indium as well as arsenic, bonds between indium and arsenic layers must be broken, we take the respective lifetimes as approximately equal with $\tau_{\text{In}} = \tau_{\text{As}} = \tau_x$. Due to desorption, the volume of the pyramid is reduced according to $dV(t)/dt = -A(t)/\tau_x$, where V and A are in units of the respective number of atoms. With $V(t=0) = V_p$, one gets $V(t) = V_p - (4/3)(\cot \alpha)^2 (t/\tau)^3$ and for the pyramid height $h(t) = h_p - (t/\tau)$. Therefore, the quantum dot lifetime becomes $t_D = (h_p - h_c) t_0 \exp(-E/k_B T)$ and represents the reduction of the dot height from initially h_p down to the critical height $h_c = 3$ ML for the 3D to 2D transition of the RHEED signals according to Ref. 3. The comparison with the experimental data for $F_{\text{As}} = 0$ yields $E_{\text{In}} = E_{\text{As}} = 3.53$ eV and $t_{0,\text{In}} = t_{0,\text{As}} = 1.14 \times 10^{-23}$ s.

In our expanded model, the pyramids consist of alternating indium and arsenic layers with index $l = 1 \dots h_p$, starting from the bottom indium layer $l = 1$. The maximum number of atoms in each layer $A_l = [2 \cot \alpha (h_p - l)]^2$ reflects the pyramid-shape. The quantity X_l describes the filling-level of the layer l and is unity directly after deposition. Desorption reduces X_l and, thus, the total island volume $V = \sum_l A_l X_l$. The filling-level evolution obeys for the indium layers

$$dX_l/dt = F_{\text{In}} - (X_l - X_{l+1})/\tau_{\text{In}}, \quad (1)$$

and for the arsenic layers

$$dX_l/dt = F_{\text{As}}(X_{l-1} - X_l) - (X_l - X_{l+1})/\tau_{\text{As}}. \quad (2)$$

These equations consider the capping of atoms in a certain layer by those in a layer over it. That means, atoms from layer l can only desorb once enough atoms from layer $l+1$ have already been removed. The set of coupled rate equations (1) and (2) is solved iteratively in order to calculate t_D in the postgrowth regime with a finite arsenic flux $F_{\text{As}} > 0$ but in the absence of an indium flux F_{In} . As described previously, t_D represents the time up to the reduction of the pyramid height down to $h_c = 3.0$ ML. Values of t_D calculated for $F_{\text{As}} = 0$ agree very well with the results of the above-mentioned continuum model.

As a very important result, the calculated t_D show a linear dependence on the arsenic flux, which is not in agreement with the experimental finding of a nearly saturated t_D at higher values of F_{As} (Fig. 3). This qualitative disagreement indicates a more complex incorporation mechanism for arsenic. In order to refine our model, we include a precursor state for the impinging As_4 molecules. Such precursor states are well established in literature for description of arsenic incorporation on GaAs surfaces.⁸ As a simplification, we assume that the precursor state is populated with arsenic atoms and that every impinging As_4 molecule produces two atoms according to the maximum sticking coefficient of 0.5. The coverage θ_{pr} of the precursor layer is given by

$$\frac{d\theta_{pr}}{dt} = F_{\text{As}}(1 - \theta_{pr}) - \frac{\theta_{pr}}{\tau_{pr}} - \frac{\theta_{pr} \left(\sum_{l=\text{As}} (X_{l-1} - X_l) \right)}{\tau_{tr}}, \quad (3)$$

where the first term describes the incorporation rate of impinging arsenic, the second term the desorption rate, and the third term the rate of transition from the precursor into the chemisorbed state prior to incorporation, with the lifetime τ_{pr} up to desorption from the precursor state and the transition lifetime τ_{tr} . The corresponding activation energies are E_{pr} and E_{tr} . As an approximation we assume that the last term in Eq. (3) is negligibly small and that θ_{pr} is in equilibrium with

$$\theta_{pr} = F_{\text{As}} / [\tau_{pr}^{-1} + F_{\text{As}}]. \quad (4)$$

To include the precursor layer in our model, F_{As} in Eq. (2) is replaced by θ_{pr}/τ_{tr} . For the analysis of the flux dependent data in Fig. 3, the remaining two parameters are determined from a fit as $\tau_{pr}(T = 518^\circ\text{C}) = 0.695$ s and $\tau_{tr}(T = 518^\circ\text{C}) = 0.00568$ s. Assuming equal prefactors for all processes, we can calculate the activation energies $E_{pr} = 3.57$ eV and $E_{tr} = 3.24$ eV. Figure 3 demonstrates the quantitative reproduction of the experimental data. As an additional important validation for the model, we calculate the temperature-dependence of t_D at a fixed arsenic flux $F_{\text{As}} = 4.8$ ML/s using the same set of parameters. The very good agreement between the calculated and the measured lifetimes, visible in Fig. 2, demonstrates the ability of our model to describe the central desorption mechanisms during the postgrowth regime.

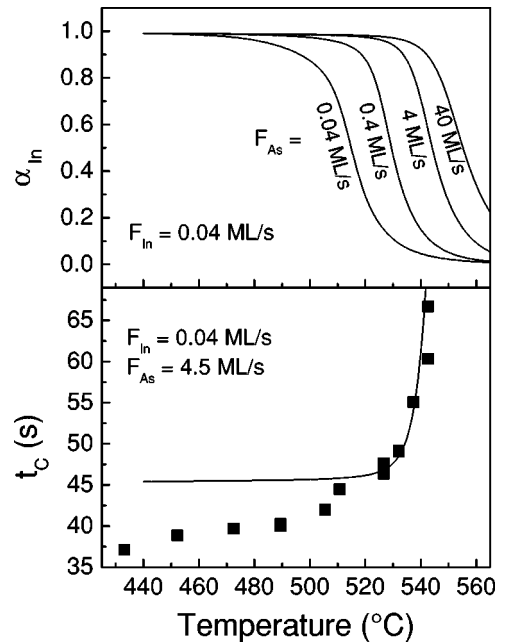


FIG. 4. The upper panel shows the calculated indium sticking coefficient α_{In} as function of the temperature at different values of the arsenic flux. In the lower panel, measured (symbols) and calculated (lines) values of the critical time t_c up to quantum dot formation are plotted vs temperature. For the calculated lines, In/Ga interdiffusion is neglected, which is important at $T < 520^\circ\text{C}$ (Ref. 3).

In further experiments, the effect of desorption during the growth process is studied. For this, we measure the time t_C up to quantum dot formation as function of the growth temperature according to Refs. 3 and 10. In these measurements $F_{\text{In}}=0.04$ ML/s, $F_{\text{As}}=4.5$ ML/s, and $T=433\text{--}548$ °C. Two regimes can be distinguished in the data: whereas up to 520 °C there is only a slight increase of t_C , at higher temperatures t_C rises very abruptly (Fig. 4). For temperatures higher than 543 °C no clear 3D growth related RHEED pattern is found. This increase of t_C with T contradicts a simple thermally activated behavior. To explain the small increase of the data up to 520 °C, we refer to Ref. 3, where this effect is attributed to segregation of gallium from the substrate into the InAs film, which reduces the effective lattice mismatch and, thus, increases t_C . The much stronger increase for $T > 520$ °C is not explainable within this picture. Here we assume that desorption comes into play.

To apply our desorption model to growth conditions, the initial conditions become $X_I(t=0)=0$. We calculate the indium sticking coefficient $\alpha_{\text{In}}=\theta_{\text{In}}/(F_{\text{In}}t)$ during 25-s deposition with $F_{\text{In}}=0.04$ ML/s and the indium coverage θ_{In} . The wetting layer is neglected in this approach. Figure 4 shows values of α_{In} calculated under variation of T for different values of F_{As} . In all cases, we find $\alpha_{\text{In}}\approx 1$ up to a certain temperature, followed by a strong decrease. A higher arsenic flux increases this transition temperature. As an example, $\alpha_{\text{In}}=0.9$ is found at $T=497$ °C for $F_{\text{As}}=0.04$ ML/s, and at $T=542$ °C for $F_{\text{As}}=40$ ML/s. These examples establish the relevance of desorption processes even at usual growth temperatures and the importance of the arsenic flux value. A reduced sticking coefficient lengthens the time that is required for the deposition of a certain

amount of material according to $t_C=t_0/\alpha_{\text{In}}$, where $F_{\text{In}}t_0$ gives the desired film thickness in the case of $\alpha_{\text{In}}=1$. This approach is applied to explain the experimental temperature-dependence of t_C at higher growth temperatures. Using $t_0=45$ s, we find good agreement as is demonstrated in Fig. 4.

As a remarkable point, the literature reports strong evidence for a temperature-dependent intermixing of the InAs quantum dots with gallium from the substrate.^{3–6} An average gallium content up to 50% in the dots can be achieved in this way. That means, in principle, desorption of both species might be of relevance. On the other hand, regarding the high activation energy for desorption of bulk-like gallium and the corresponding high temperatures of at least 750 °C,¹³ we assume that gallium desorption is not relevant at the temperatures considered here. This is supported by our experimental finding of only one activation energy as is visible in the temperature-dependence of t_D (Fig. 2).

Our results establish the importance of desorption processes that cannot be neglected during growth of self-assembled InAs quantum dots at the technologically relevant temperatures. In particular, desorption of indium causes two effects: first the total amount of material stored in the quantum dots will be reduced and second the dots become more gallium rich. Both effects crucially modify the electronic properties of the quantum dots. A sufficient arsenic flux reduces the indium desorption and, thus, enhances the indium sticking coefficient and the postgrowth quantum dot lifetime.

The author would like to thank S. Mendach and W. Hansen for very helpful discussions, C. Weichsel for AFM measurements, and the “Deutsche Forschungsgemeinschaft” for financial support via HA 2042/3 and via SFB 508.

*E-mail: heyn@physnet.uni-hamburg.de

¹D. Bimberg, M. Grundmann, and N. N. Ledentsov, *Quantum Dot Heterostructures*, (Wiley, Chichester, 1999).

²L. Chu, M. Arzberger, G. Böhm, and G. Abstreiter, *J. Appl. Phys.* **85**, 2355 (1999).

³Ch. Heyn, *Phys. Rev. B* **64**, 165306 (2001).

⁴P.B. Joyce, T.J. Krzyzewski, G.R. Bell, B.A. Joyce, and T.S. Jones, *Phys. Rev. B* **58**, R15 981 (1998).

⁵K. Zhang, Ch. Heyn, W. Hansen, Th. Schmidt, and J. Falta, *Appl. Phys. Lett.* **77**, 1295 (2000).

⁶I. Kegel, T.H. Metzger, A. Lorke, J. Peisl, J. Stangl, G. Bauer, J.M. Garcia, and P.M. Petroff, *Phys. Rev. Lett.* **85**, 1694 (2000).

⁷Ch. Heyn and M. Harsdorff, *Appl. Surf. Sci.* **100/101**, 494 (1996).

⁸C.T. Foxon and B.A. Joyce, *Surf. Sci.* **50**, 434 (1975).

⁹H. Lee, R. Lowe-Webb, W. Yang, and P.C. Sercel, *Appl. Phys. Lett.* **72**, 812 (1998).

¹⁰Ch. Heyn, D. Endler, K. Zhang, and W. Hansen, *J. Cryst. Growth* **210**, 421 (2000).

¹¹C. Sasaoka, Y. Kato, and A. Usui, *Appl. Phys. Lett.* **62**, 2338 (1993).

¹²J. Marquez, L. Geelhaar, and K. Jacobi, *Appl. Phys. Lett.* **78**, 2309 (2001).

¹³N. Sugiyama, T. Isu, and J. Katayama, *Jpn. J. Appl. Phys., Part 2* **28**, L287 (1989).